Particle velocity and flow development in a long and high-flux circulating fluidized bed riser

J. H. Pärssinen [1], J.-X. Zhu [*]

Department of Chemical and Biochemical Engineering, University of Western Ontario, London, Ont., Canada N6A 5B9

Abstract

In a 10 m tall and 76 mm i.d. high-flux riser, radial profiles of particle velocities were determined with a five-fiber optic probe on seven axial levels, with solids circulation rate (solids flux) up to 550 kg/m^{2}s and superficial gas velocity up to 10 m/s. This study shows a more comprehensive set of radial profiles under higher fluxes than any previous literature. Four axial stages of flow development were distinguished based on radial distributions of particle velocity and concentration. Compared to low-flux operations (< 200 kg/m^{2}s), the radial profiles of particle velocity are significantly less uniform at high-flux operations (> 300 kg/m^{2}s). The superficial gas velocity has more influence on the radial velocity profiles than the solids flux at high solids flux. Net solids downflow only occurs near the wall under limited conditions in the bottom section. © 2001 Elsevier Science Ltd. All rights reserved.

Keywords: Circulating fluidized bed; Radial particle velocity profile; High solids circulation rate; Five-fiber optic probe

1. Introduction

Circulating fluidized beds have been studied intensively during the past decades in order to improve some industrial processes, such as CFB combustion and fluid-catalytic cracking (FCC). FCC units are used in most refineries all over the world to convert high molecular-weight gas oils or residuum charge stocks into lighter hydrocarbon products in a riser reactor within a few seconds. However, a shorter and a more uniform catalyst residence time in the riser reactor would potentially lead to a better reaction performance (larger amounts of desired products and/or a higher conversion). That is because coke deposition rapidly deactivates the catalyst leading to reduced selectivity and some desirable products (gasoline, light olefins, light cycle oil) may react further causing over-cracking. These non-beneficial factors could, however, be limited or avoided by having a more uniform axial and radial particle flow structure in the riser, leading to shorter and more uniform solids (and gas) residence times.

To properly model, design and optimize the catalyst flow in a commercial scale riser, it would be helpful to obtain fundamental knowledge from pilot scale risers operated under similar solids fluxes. However, most previous studies were carried out under low solids fluxes less than 200 kg/m^{2}s, whereas the industrial range is from 400 to 1200 kg/m^{2}s in FCC risers (Zhu & Bi, 1995). On the other hand, recent studies under high solids flux (Issangya, Bai, Grace, Lim, & Zhu, 1997a; Issangya et al., 1997b, 1999; Issangya, Bai, Grace, & Zhu, 1998, 2000; Grace et al., 1999; Karri & Knowlton, 1999; Pärssinen & Zhu, 2001) have shown that the hydrodynamics are quite different under higher fluxes and high suspension densities compared to low-flux and low-density risers operated with G_s of 200 kg/m^{2}s or less. Before the above studies, only very limited studies in the previous literature were conducted under extremely high solids fluxes ranged beyond 500 kg/m^{2}s (van Zoonen, 1962; Azzi et al., 1991; Martin et al., 1992; Contractor et al., 1994; Knowlton, 1995; van Landgenem et al., 1995; Pugsley, Milne, & Berruti, 1996).

Although there have been some studies on risers with high solids flux, there is still a lack of experimental

----

[*] Corresponding author. Tel.: +1-519-661-3807; fax: +1-519-661-2441.

E-mail address: zhu@uwo.ca (J.-X. Zhu).

[1] Visiting from Helsinki University of Technology, Sähkömiehentie 4A, 02150 Espoo, Finland.
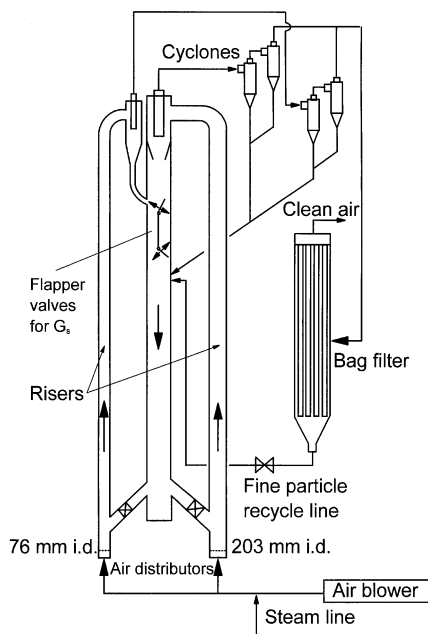
Fig. 1. A schematic diagram of the twin-riser circulating fluidized bed apparatus.

high-flux data, especially on particle velocities. For example, no previous study has shown the radial and axial particle velocity profiles over a wide range of high-flux operating conditions. Therefore, this study was carried out to gain a solid understanding and knowledge of flow development regarding radial and axial profiles of particle velocity under very high solids fluxes up to $550 \, \text{kg/m}^2\text{s}$. In addition to the FCC process, there are also some rising applications of high-flux CFB such as duPont's production of maleic anhydride (Contractor et al., 1994), which will also benefit from this study.

2. Experimental apparatus

The experiments were conducted in a circulating fluidized bed system that is schematically shown in Fig. 1. The system consists of two 10 m long risers, which utilize the same downcomer with an internal diameter of 0.32 m. The internal diameters of the risers were 76 and 203 mm, but for the current work the measurements were done only in the 76 mm i.d. riser when the 203 mm riser was not in operation. The solids were FCC catalysts with a mean diameter of 67 μm and a particle density of $1500 \, \text{kg/m}^3$. The humidity level of the air was controlled between 70% and 80% to eliminate the electrostatics in the system.

After passing a short inclined pipe section, the solids entered the riser bottom at the height of 0.17–0.25 m and were accelerated by air in ambient conditions.

After initial mixing and acceleration, the solids started their travel up in the column. In the riser top, the solids passed the smooth exit into the primary cyclone for gas-solids separation, and some escaped solids entered into the secondary and tertiary cyclones, whereafter the final gas-solids separation was carried out in a bag filter. From the bottom of the large capacity bag filter, fine particles that were collected could be returned back into the downcomer. The solids flow rate measuring device located at the top portion of the downcomer sectioned the column into two halves with a central vertical plate and with two half butterfly valves fixed at the top and the bottom of the two-half section. By appropriately flipping over the two valves from one side to the other, solids circulated through the system can be accumulated on one side of the measuring section for a given time period to provide the solids circulation rate.

A five-fiber optic velocity probe was inserted into the column to measure the particle velocity. The five-fiber optic probe consists of two light emitting fibers (B and D) and three light detecting fibers (A, C and E) arranged precisely in the same line. A particle flowing by the center point between any two neighboring fibers will produce a reflective signal to a detection fiber. By counting the time difference between the two signals from A–B and B–C (or C–D and D–E), the velocity of a particle passing along the array of the five fibers can be determined. This probe does not have a fixed sampling frequency, but samples every particle flowing by and reports all qualified measurements. More details of the five-fiber optic probe have been presented elsewhere (Zhu et al., 2001). The particle velocity was measured on seven axial levels ($z = 1.53$, 2.73, 3.96, 5.13, 6.34, 8.74 and 9.42 m) and at 11 radial positions ($r/R = 0.00$, 0.16, 0.38, 0.50, 0.59, 0.67, 0.74, 0.81, 0.87, 0.92 and 0.98) on each level. At each measurement location, the sampling time was typically over 30 s, which gives a minimum of 2500 sampled particles.

Solids concentration measurements were conducted with a reflective-type fiber optic concentration probe. The 3.8 mm diameter probe tip consisted of approximately 8000 emitting and receiving quartz fibers, each having a diameter of 15 μm. The active area, where the fibers were located, was approximately 2 mm × 2 mm. More details of this probe can be found in Zhang, Johnston, Zhu, Lasa, and Bergougnou (1998), and more details of the concentration probe measurements from the same riser can be found in Pärssinen and Zhu (2001). By combining the results from the current study with those of Pärssinen and Zhu (2001), the cross-sectional net solids fluxes were obtained for each axial elevation. Those were found to be in good agreement with the results from the solids flowrate measuring device (G_s) in the downcomer (within 10–15%).
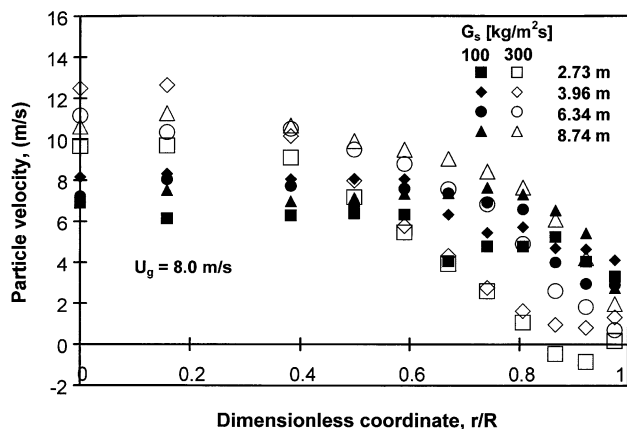
Fig. 2. A comparison of the particle velocity profiles between low-flux ($G_s = 100$ kg/m^{2}s) and high-flux ($G_s = 300$ kg/m^{2}s) operating conditions at a constant $U_g = 8$ m/s.

3. Results and discussion

3.1. Comparison of low-flux and high-flux velocity profiles

Fig. 2 compares the radial distributions of particle velocity between a low-flux ($G_s = 100$ kg/m^{2}s) and a high-flux ($G_s = 300$ kg/m^{2}s) condition under a constant U_g of 8 m/s. Under the low flux, the radial distributions of particle velocity are comparably more uniform and less sensitive to the change of the axial position. The latter is most likely due to the quick flow development under low flux, as will be further discussed later. On the other hand, flow development is much slower under high flux so that the radial profile continues to change in Fig. 2.

Fig. 2 also shows unexpectedly that the particle velocities are higher in the riser center for the higher flux of 300 kg/m^{2}s, compared to the low flux of 100 kg/m^{2}s. This could be explained by the fact that under a higher G_s (with a constant U_g) a denser concentration of solids occupies the wall region (see Pärssinen & Zhu, 2001) and restricts the gas flow. In order to maintain the cross-sectional U_g of 8 m/s, the gas velocity has to be correspondingly higher in the riser center (see also van Breugel, Stein, & de Vries, 1969; Martin et al., 1992; Liu, Grace, Bi, Morikawa, & Zhu, 1999). A higher gas velocity in the center could also lead to higher particle velocities, as long as the solids holdup (concentration) in the center does not increase significantly with increasing G_s (because a much higher solids concentration would increase solids aggregation which would in turn increase the slip velocity and therefore lower the local particle velocity). However, Pärssinen and Zhu (2001) have shown that the solids concentration remained nearly constant r/R from 0.0 to 0.632 with increasing G_s under a constant U_g so that there is no increased particle ag-

gregation (clustering) in the riser center for the higher G_s of 300 kg/m^{2}s. Knowlton (1995) also indicated that the particle velocity was higher in the riser center for a higher G_s of 489 kg/m^{2}s compared to G_s of 196 kg/m^{2}s under a constant U_g of 11 m/s, in good agreement with our results here. On the other hand, partly for the same reasons as discussed above (solids aggregation and/or radial gas flow profile) the particle velocities tend to be lower in the wall region for G_s of 300 kg/m^{2}s compared to G_s of 100 kg/m^{2}s. When G_s was increased to 400 kg/m^{2}s and then to 550 kg/m^{2}s at U_g of 8.0 m/s, the particle velocities were found to remain low in the wall but increased further at the riser axis.

The above phenomenon suggests that low-flux data have very limited usefulness for high-flux flow modeling. In addition, the solids flow direction in the wall region of a low-flux riser is often reported to be downwards under fluxes of less than 200 kg/m^{2}s and superficial gas velocities of less than 6.5 m/s (Bader, Findlay, & Knowlton, 1988; Glicksman, 1988; Hartge, Rensner, & Werther, 1988; Nowak, Mineo, Yamazaki, & Yoshida, 1991), in contrast to high-flux and/or high-density applications where the flow direction is nearly always upwards (Grace et al., 1999). This also makes the data obtained under low-flux conditions less useful, so that there is clearly a need to conduct research under higher G_s.

3.2. Axial development of particle velocities

Fig. 3 shows the one-dimensional (cross-sectional average) particle velocities on seven axial levels obtained with the fiber optic velocity (Fig. 3a) and concentration (Fig. 3b) probes. In Fig. 3a, the local particle velocity was weighted with the local solids holdup in each position to give the true cross-sectional average velocity since a higher solids population is typically flowing near the wall than in the center. In Fig. 3b, the cross-sectionally averaged solids concentration (Pärssinen and Zhu, 2001) was used to calculate the average particle velocity ($= G_s/(\rho_p \bar{\varepsilon}_s)$). The excellent agreement (both average deviation of less than 10%) between Figs. 3a and b further confirms the reliability of the two optical fiber probes used in this study.

In an early paper by the same authors reporting on the axial distributions of solids holdup, Pärssinen and Zhu (2001) found four axial sections along the high-flux riser: (1) the bottom dense section with solids holdups of about 20% or higher, (2) a middle section with intermediate solids holdups of about 7–8% to 15–20%, (3) a dilute section where the holdup is typically about 3–5% and (4) a top exit section where the holdup is somewhat higher than the dilute section due to the minor exit effect. Such a four-section structure can also be observed in the axial profiles of the one-dimensional particle velocity shown in
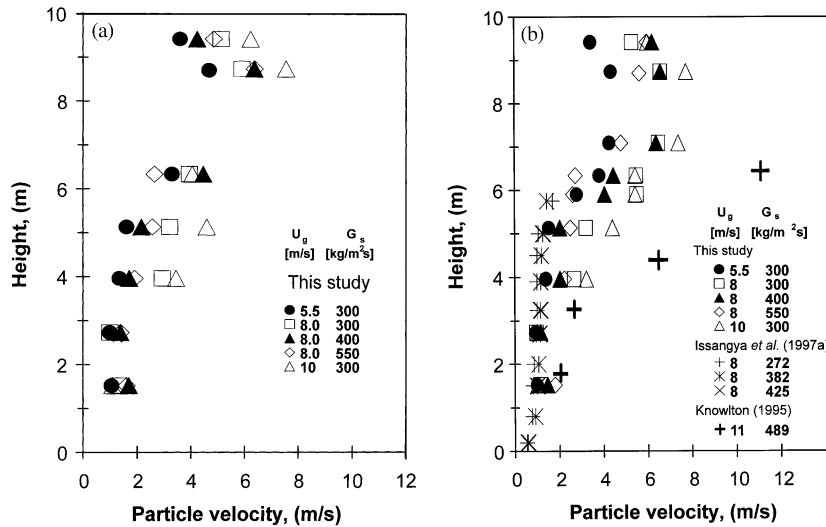
Fig. 3. Axial profiles of one-dimensional particle velocity under high solids fluxes: (a) averaged from local particle velocities (weighed by local solids concentration); (b) deferred from the cross-sectional average solids concentration.

Fig. 3. In the bottom dense section (below 3–4 m), there is no obvious solids acceleration and the particle velocity is typically less than 2 m/s. Around 3–4 m, particles begin to accelerate significantly. In this middle intermediate dense section whose length decreases with gas velocity and increases with solids flux, particle velocity ranges approximately from 2 to 4 m/s. Depending on the operating conditions, the upper dilute section appears at a level of 5–7 m and extends to around a level of 9 m where the typical particle velocities reach within 2–3 m/s of their respective gas velocities. In the top exit region, there is a reduction of particle velocity due to the minor exit effect.

To compare with results from previous literature, solids concentration data from Issangya et al. (1997a) and Knowlton (1995) are also converted to one-dimensional particle velocity and plotted in Fig. 3b. Fig. 3b indicates that the results of Issangya et al. (1997a) are not very similar to ours, in that their middle intermediate dense section is much longer and its particle velocity much lower due to the very high solids holdup in that section. This is due to the large solids inventory and the larger downcomer-to-riser height ratio, as discussed by Pärssinen and Zhu (2001). Since their riser is short, the dilute section was only present near the top of their riser of 6.3 m for limited conditions. The axial velocity profile of Knowlton (1995) is similar to our results but with higher particle velocities at each level apparently due to the high gas velocity.

3.3. Development of radial profiles of particle velocity

In Fig. 4 the profiles of radial particle velocity on seven axial elevations under five high-flux operating conditions

are collected. The solids circulation rates were 300, 400 and 550 $kg/m^2 s$ and the superficial gas velocity 5.5, 8.0 and 10.0 m/s. Fig. 4 also shows the four stages of flow development, as shown by Fig. 3, but with respect to the radial profiles of particle velocity under each operating condition in the 10 m high riser. At the bottom dense section ($z = 1.53$ m and/or 2.73 m) the radial profile shows a flat center region, then turning smoothly downward towards the wall, and having a fairly wide wall region with a velocity value of less than 2 m/s (upwards). This may be referred to as a horizontal "S" shape. In the middle intermediate dense section, the solids accelerate more in the radial region of $r/R = 0.0$–0.4, leading to a nearly linear (but not flat) radial velocity profile. This second stage, typically observed between the heights of 2.73 and 5.13 m, can occupy a relatively long portion of the riser, if the solids loading ratio is high (ratio of G_s–U_g). The third section, where the radial profiles change from the linear shape to a parabolic shape, takes place somewhere between the heights of 5.13–8.74 m, depending on the operating conditions. When the solids reach the exit section (fourth stage) the particles slow down somewhat, and the corresponding velocity profiles become scattered, due to the exit features as the solids pass through the 90° smooth elbow.

These four stages of flow development are clearly present for all high-flux operating conditions in our 10 m high riser. The existence and the respective length of each section are dependent on the operating conditions. Fig. 5 shows that increasing U_g from 5.5 to 8.0 m/s and then to 10.0 m/s (with $G_s = 300 kg/m^2 s$) causes stages two and three to start at lower axial levels, suggesting a faster flow development. Fig. 5 also clearly shows a faster flow development for the higher U_g of 8.0 and
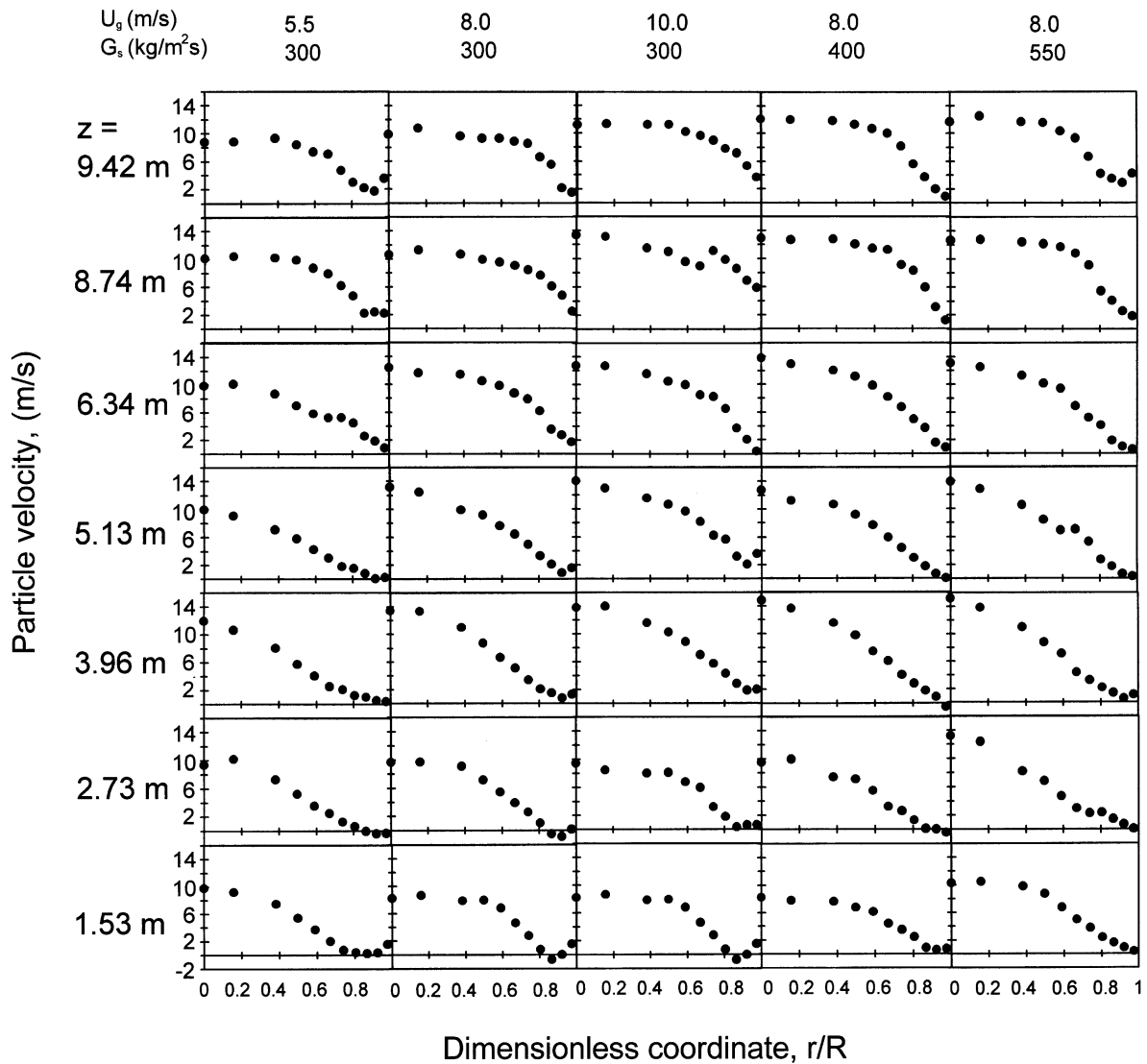
Fig. 4. Radial profiles of particle velocity under all high-flux operating conditions, showing the flow development along the riser.

10.0 m/s by comparing the velocity profiles at 1.53, 2.73 and 3.96 m (marked as closed symbols with connecting lines). On the other hand, increasing G_s does not seem to change the development patterns significantly under a constant U_g of 8.0 m/s (Fig. 4).

When observing the radial profiles towards the riser top, it is also seen that the flow develops first in the riser center region, and then gradually and progressively closer to the wall as the solids pass through the riser. This can be seen more clearly in Fig. 6 which plots the local particle velocities in various radial regions on six axial elevations in the riser. In this figure, the difference in the flow development in the three radial regions is clearly revealed. In the riser center ($r/R = 0.0–0.632$) the particles already gained a fairly high velocity before the height of 1.5 m, whereas a maximum velocity is finally reached at the height of 3–4 m, except from the lowest U_g

of 5.5 m/s for which the velocity still increases slightly in the upper portion of the riser. In the middle region ($r/R = 0.632–0.894$), on the other hand, the particle velocity is increasing throughout the riser, but with the most significant change in the 5–7 m section. In the wall region ($r/R = 0.894–1.0$) the particle velocity remains low up to about 6 m and then increases slowly towards the riser top.

Fig. 6 clearly shows that particle acceleration (therefore flow development) first starts from the center and then extends to the wall. This dictates the development of the radial profiles of particle velocity. In the bottom dense section, only those particles in the center region have had some acceleration so that the horizontal S shape appears. In the middle section, particles in the middle radial region start to accelerate so that the particle velocity in this region increases, resulting in the nearly linear
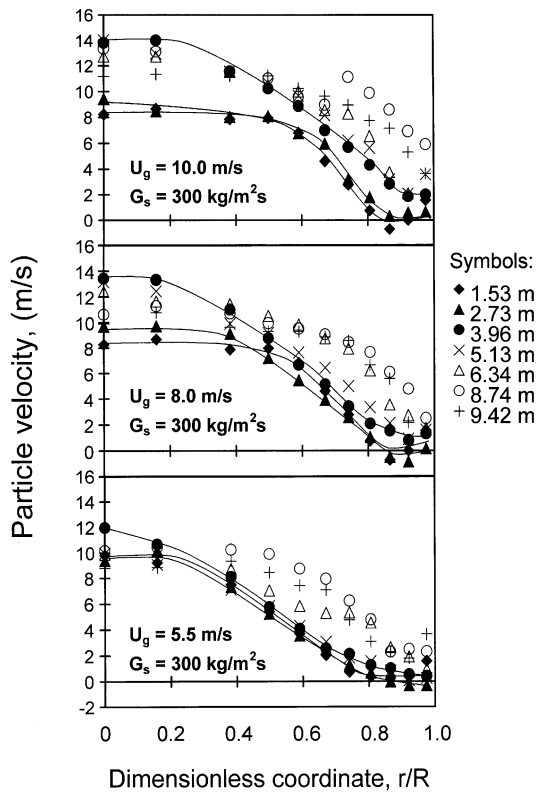
Fig. 5. Development of radial profiles of local particle velocities along the riser for $G_s = 300$ kg/m^{2}s at gas velocities of $U_g = 5.5$, 8.0 and 10.0 m/s.
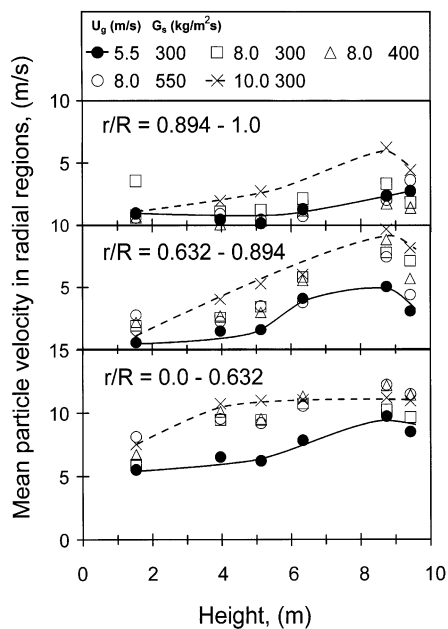
Fig. 6. Particle acceleration in different radial regions along the riser under all five high-flux operating conditions.

increasing velocity profile from the wall. In the upper dilute section, particles in the middle region accelerate further to catch up with those particles in the center, and particles in the wall region also begin to accelerate, leading to a parabolic radial profile.

Fig. 6 also indicates that an increase in the gas velocity significantly enhances the flow development (i.e., to cause particles to accelerate quicker and at lower levels in the riser) while increasing solids circulation rate under high-flux conditions does not seem to affect particle acceleration, in agreement with the observations from Figs. 4 and 5. However, decreasing the solids circulation rate from 300 kg/m^{2}s under the same gas velocity does significantly accelerate the flow development, as shown in Fig. 2, so that the radial distribution of particle velocity reaches a stable parabolic shape quickly. Zhou et al. (1995) has also observed that, under low flux conditions, an increase in the solids circulation rate leads to steeper radial profiles for particle velocity.

Fig. 7 provides the typical radial profiles of particle velocity in the three axial sections (excluding the exit section), by averaging the local velocity values at each axial elevation within the respective sections. As expected, three distinct radial profiles are shown for the three radial sections, a horizontal S shape in the bottom, a linear profile in the middle and parabolic in the top section. Fig. 7 also shows that increasing U_g tends to make the normalized radial profiles more uniform while changing G_s does not seem to affect the radial profiles. These averaged typical profiles offer very useful information for high-flux flow modeling and may be used to replace the oversimplified plug flow or core-annulus flow assumptions.

Figs. 4–7 all show that particles near the wall mostly flow upwards in a high-flux riser, different from most reported results from low-flux risers (e.g., Zhou et al., 1995). This is because both solids concentration and flux are high in the high-flux riser, significantly impeding the tendency of particle downflow in the wall region (Grace et al., 1999). Such net upflow in the wall region seems to be typical of a high-flux and/or high-density operation.

3.4. Particle velocities vs. solids holdups

Fig. 8 shows the variation of particle velocity in the wall region with the cross-sectional mean solids holdup. It can be seen that under high-flux conditions ($G_s \geqslant 300$ kg/m^{2}s) the particles mostly flow upwards at the riser wall. The particle velocity in the wall region could also be related rather well to the cross-sectional solids concentration at each axial level, as shown in Fig. 8. With a lower cross-sectional solids concentration (riser top), the particle velocities are higher, often over 2 m/s, at the wall. With a high cross-sectional mean
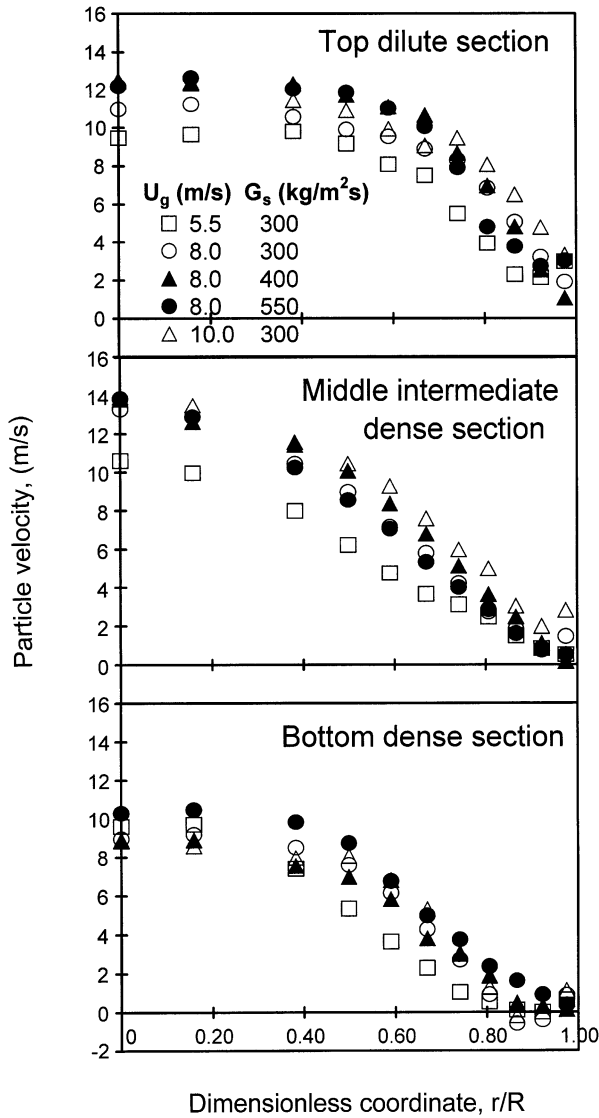
Fig. 7. Typical radial profiles of particle velocity in the three axial sections along the riser.

Fig. 8. Relationship between the particle velocity at the riser wall ($r/R = 0.92$ and 0.98) and the cross-sectional solids holdup on all seven axial elevations under all five high-flux operating conditions.
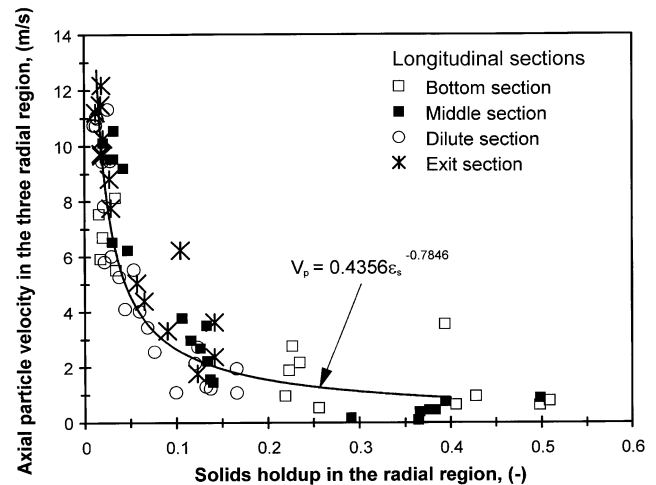
Fig. 9. Relationship between the average particle velocity and the average local solids holdup in the three radial regions ($r/R = 0.0$–0.632, 0.632–0.894 and 0.894–1.0) throughout the high-flux riser.

solids concentration (riser bottom), the mean particle velocity is typically around 1 m/s. A simple regression provides the following correlation between the particle velocity at the wall and the cross-sectional average solids holdup.

$$V_{p,\text{wall}} = -1.1827\ln(\bar{\varepsilon}_s) - 1.5467. \qquad (1)$$

Similar to what is found here, Grace et al. (1999) pointed out that the net flow direction is upwards at the wall of a high-density riser (cross-sectional solids concentration over 10%). For their high-flux riser, Knowlton (1995) and Karri and Knowlton (1999) also suggested that the flow direction is upwards (when $U_g > 5$ m/s), although the operation did not fulfill the definition of a high-density riser (Grace et al., 1999).

The average local particle velocity in the three radial regions ($r/R = 0.0$–0.632, 0.632–0.894 and 0.894–1.0) at a given axial position can also be directly related to the average local solids concentration throughout our high-flux riser. As shown in Fig. 9, the local average particle velocity decreases monotonically with the local solids concentration and such a decrease follows the same pattern in all four axial sections. Such a strong dependence could only be understood by considering solids aggregation at each local position: a higher solids concentration leads to stronger particle aggregates, resulting in a lower effective drag between the particles and gas, and therefore a lower particle velocity under a constant gas velocity. The independence of the above variation with the axial locations shows the inherent connection between the particle concentration and velocity. As a result, a single correlation

works for all axial sections

$$V_p = 0.4356\varepsilon_s^{-0.7846}. \tag{2}$$

3.5. High-flux vs. high-density operation

By comparing our findings with previous literature, it can be concluded that a high-flux riser could be operated with longitudinal regions of only (1), (2) and (4) (Issangya et al., 1997a; 1997b; 1998; 1999; 2000; Issangya, 1998), if there is a high total solids inventory and the riser is relatively short. This could be referred to as a truly high-density riser as long as the solids concentration exceeds 10% throughout the riser (Grace et al., 1999). On the other hand, in the studies of Knowlton (1995) and Karri and Knowlton (1999) and ours, all these four longitudinal regions have been established, due to a longer riser (14.2 and 10 m) and a relatively lower solids inventory. Since the solids flow direction is upwards in the wall region throughout the riser, and there is no clear core-annulus flow structure (Karri & Knowlton, 1999; current study), the hydrodynamics does not correspond well to the conventional definition of fast fluidization, typically observed in conjunction with lower solids fluxes (G_s of 200 kg/m²s or less). On the other hand, due to a lower solids concentration ($< 10\%$) in the dilute region, our findings do not match well with the high-density concept either. Whether a new flow regime should be defined for high-flux operating conditions (and CFB systems) such as ours is left for future research since more data are needed for such a classification.

4. Conclusions

A comprehensive mapping of flow development and particle velocities were shown for the first time in the literature for the solids flow in a long riser at high solids fluxes up to 550 kg/m²s. Four longitudinal sections were shown to exist: bottom dense section, middle intermediate dense section, dilute section, and exit section. The corresponding radial profiles in these four sections are: S-shape in the bottom dense section, linear (but not flat) in the middle section, parabolic in the dilute section, and eventually, parabolic with some scattering in the exit section. The dilute section sometimes disappears, depending on the overall pressure balance around the system, the catalyst inventory, the pressure loss over the solids control valve, giving the high-density operation.

By increasing U_g, the flow development was shown to become faster. A decrease in G_s also has a similar effect for G_s from 100 to 300 kg/m²s, but little influence when $G_s \geqslant 300$ kg/m²s. The flow develops first in the riser center ($r/R = 0.0$–0.632), within the bottom dense region below the height of 4 m, and then gradually closer to the wall as the solids pass through the riser. In the middle ra-

dial region, the increase in particle velocity is strikingly large and continues throughout the column, whereas in the wall region the particles only start to accelerate in the dilute region. The solids flow direction at the wall was found to be upward (on average) and typically less than 2 m/s.

In all the locations measured, there was a clear dependence between the local particle velocity and concentration. Particle aggregation is considered as one of the key factors that affects the local hydrodynamics in the high-flux riser.

Notation

G_s	solids circulation rate (solids flux), kg/m²s
r	radial distance from riser axis, m
R	radius of riser, m
U_g	superficial gas velocity, m/s
V_p	particle velocity, m/s
$V_{p,\text{wall}}$	particle velocity in the wall region, m/s
z	height from the riser bottom, m
$\bar{\varepsilon}_s$	cross-sectional mean solids holdup, dimensionless

References

Azzi, M., Turlier, P., & Betrand, J. R. (1991). Mapping solids concentration in a circulating fluidized bed using gammametry, *Powder Technology*, *67*, 249–258.

Bader, R., Findlay, J., & Knowlton, T. M. (1988). Gas/solid flow patterns in a 30.5 cm-diameter circulating fluidized bed. In P. Basu, & J. F. Large (Eds.), *Circulating fluidized bed technology II* (pp. 123–137). Oxford: Pergamon Press.

Contractor, R. M., Patience, G. S., Garnett, D. I., Horowitz, H. S., Sisler, G. M., & Bergna, H. E. (1994). In A. Avidan (Ed.), *Circulating fluidized bed technology IV* (pp. 387–391). New York: American Institute of Chemical Engineers.

Glicksman, L. R. (1988). Circulating fluidized bed heat transfer. In P. Basu, & J. F. Large (Eds.), *Circulating fluidized bed technology II* (pp. 13–29) Oxford: Pergamon Press.

Grace, J. R., Issangya, A. S., Bai, D., Bi, H.-T., & Zhu, J.-X. (1999). Situating the high-density circulating fluidized bed. *A.I.Ch.E. Journal*, *45*, 2108–2116.

Hartge, E. U., Rensner, D., & Werther, J. (1988). Solids concentration and velocity patterns in circulating fluidized beds. In P. Basu, & J. F. Large (Eds.), *Circulating fluidized bed technology II* (pp. 165–180). Oxford: Pergamon Press.

Issangya, A. S., Bai, D., Grace, J. R., Lim, K. S., & Zhu, J. (1997a). Flow behaviour in the riser of a high-density circulating fluidized bed. *A.I.Ch.E. Symposium Series*, *93*(317), 25–30.

Issangya, A. S., Bai, D., Bi, H. T., Lim, K. S., Zhu, J., & Grace, J. R. (1997b). Axial solids holdup profiles in a high-density circulating fluidized bed riser. In M. Kwauk, & J. Li (Eds.), *Circulating fluidized bed technology V* (pp. 60–65). Beijing: Science Press.

Issangya, A. S. (1998). Flow dynamics in high density circulating fluidized beds. *Ph.D. Dissertation*, University of British Columbia, Vancouver, BC.

Issangya, A. S., Bai, D., Grace, J. R., & Zhu, J. (1998). Solids flux profiles in a high density circulating fluidized bed riser. In L. S. Fan, & T. M. Knowlton (Eds.), *Fluidization IX* (pp. 197–204). New York: Engineering Foundation.

Issangya, A. S., Bai, D., Bi, H. T., Lim, K. S., Zhu, J., & Grace, J. R. (1999). Suspension densities in a high-density circulating fluidized bed riser. *Chemical Engineering Science*, *54*, 5451–5460.

Issangya, A. S., Grace, J. R., Bai, D., & Zhu, J. (2000). Further measurements of flow dynamics in a high-density circulating fluidized bed riser. *Powder Technology*, *111*, 104–113.

Karri, S. B. R., & Knowlton, T. M. (1999). A comparison of annulus solids flow direction and radial solids mass flux profiles at low and high mass fluxes in a riser. In J. Werther (Ed.), *Circulating fluidized bed technology VI* (pp. 71–76). Frankfurt: Dechema.

Knowlton, T. (1995). *Interaction of pressure and diameter on CFB pressure drop and holdup. Paper for workshop*: Modeling and control of fluidized bed systems, Hamburg, May 22–23.

Liu, J., Grace, J. R., Bi, H., Morikawa, H., & Zhu, J. (1999). Gas dispersion in fast fluidization and dense suspension upflow. *Chemical Engineering Science*, *54*, 5441–5449.

Martin, M. P., Turlier, P., & Bernard, J. R. (1992). Gas and solid behaviour in cracking circulating fluidized beds. *Powder Technology*, *70*, 249–258.

Nowak, W., Mineo, H., Yamazaki, R., & Yoshida, K. (1991). Behavior of particles in a circulating fluidized bed of a mixture of two different sized particles. In P. Basu, M. Horio, & M. Hasatani (Eds.), *Circulating fluidized bed technology III* (pp. 219–224). Oxford: Pergamon Press.

Pärssinen, J. H., & Zhu, J.-X. (2001). Axial and radial solids distributions in a long and high-flux CFB riser. *A.I.Ch.E. Journal*, in press.

Pugsley, T. S., Milne, B. J., & Berruti, F. (1996). An innovative non-mechanical solids feeder for high solids mass fluxes in circulating fluidized bed risers. *Powder Technology*, *88*, 123–131.

van Breugel, J. W., Stein, J. J. M., & de Vries, R. J. (1969). Isokinetic sampling in a dense gas-solids stream. *Proceedings of the institution of mechanical engineers*, *184*, 18–23.

van Landgenem, F., Nevicato, D., Pitault, I., Forissier, M., Turlier, P., Derouin, C., & Bernard, J. R. (1995). Fluid catalytic cracking: modelling of an industrial riser. *Applied Catalysis A: General*, *138*, 381–405.

van Zoonen, D. (1962), Measurement of diffusional phenomena and velocity profiles in a vertical riser. *Proceeding of the Symposium on the Interaction between Fluids and Particles*, London (pp. 64–71).

Zhang, H., Johnston, P. M., Zhu, J.-X., de Lasa, H. I., & Bergougnou, M. A. (1998). A novel calibration procedure for a fibre optic concentration probe. *Powder Technology*, *100*, 260–272.

Zhou, J., Grace, J. R., Brereton, C., & Lim, C. J. (1995). Particle velocity profiles in a circulating fluidized bed of square cross-section. *Chemical Engineering Science*, *50*, 237–244.

Zhu, J.-X., & Bi, H.-T. (1995). Distinctions between low density and high density circulating fluidized beds. *Canadian Journal of Chemical Engineering*, *73*, 644–649.

Zhu, J.-X., Li, G-Z., Qin, S-Z., Li, F-Y., Zhang, H., & Yang, Y-L. (2001). Direct measurements of particle velocities in gas–solids suspension flow using a novel 5-fiber optical probe. *Powder Technology*, *115*(2), 184–192.